Reduction of miR-29a-3p induced cardiac ischemia reperfusion injury in mice via targeting Bax

LIANG ZHANG, JIAN ZHANG, QIGUANG TONG, GUANNAN WANG, HONGLING DONG,
ZHONGLU WANG, QI SUN and HANGYU WU

Heart Center, Beijing Chest Hospital, Capital Medical University, Beijing 101149, P.R. China

Abstract. The current study mainly aimed to evaluate the expression and the potential mechanism of miR-29a-3p in the hearts of mice after cardiac ischemia reperfusion (CIR) injury. Quantitative PCR was carried out to assess the relative levels of miR-29a-3p in the hearts of a CIR injury mouse model. To the best of our knowledge, the current study is the first to show that the level of miR-29a-3p was significantly decreased in the hearts of CIR injury mouse models compared with that of sham controls. Moreover, the authors found that decreased miR-29a-3p levels enhanced the production of reactive oxygen species in cardiomyocytes. Meanwhile, the inhibition of miR-29a-3p induced substantial cardiomyocyte apoptosis. Further study showed that the inhibition of miR-29a-3p decreased the activation of Akt and p38, suggesting a stress-induced self-regulatory mechanism after CIR injury in primary cardiomyocytes. A dual luciferase assay and western blot analysis showed that Bax was a target gene of miR-29a-3p. The authors also measured the level of miR-29a-3p in the plasma of 100 acute myocardial infarction (AMI) patients and found that circulating miR-29a-3p was significantly decreased in AMI patients. Receiver operating characteristic curve analysis showed that miR-29a-3p could be used to screen AMI patients from healthy controls. Hence, the authors of the current study propose that reduced miR-29a-3p levels in primary cardiomyocytes contribute to CIR injury-related apoptosis mainly by targeting Bax.

Introduction

Due to sustained ischemia, myocardial infarction (MI) is pathologically characterized by myocardial cell death and is known as the most severe manifestation of coronary artery disease (CAD) (1,2). It is estimated that over seven million deaths globally are caused by CAD each year (3). Generally, the progression of CAD is chronic, and is accompanied by the erosion of the endothelium and the buildup of plaque, thereby gradually narrowing the coronary artery (4). Once the plaque suffers a sudden rupture and AMI may occur, which is a serious threat to human health (4). Sustained ischemia results in decreased heart contractility since myocardial cells have a relatively poor proliferation ability (5). Hence, it is important to re-vascularize the occluded artery for MI therapy.

In the pathogenesis of myocardial infarction, cardiac cell death has been suggested to contribute to terminal differentiation and the loss of regenerative capacity (6). Apoptosis is one of the main types of cell death processes, and it occurs through interactions with death receptors (7). Multiple pro-apoptosis and/or anti-apoptosis factors, including members of the caspase family, the Bcl-2 family, cytochrome c and p53, have been suggested to be involved in the signal transduction of apoptosis (2,8,9).

Recently, increasing evidence has demonstrated the importance of microRNAs (known as miRNAs or miRs) in modulating apoptosis, necroptosis and autophagy in cardiomyocytes, thereby regulating the progression of myocardial infarction (10,11). For instance, miR-1 contributes to cardiac ischemia reperfusion injury by targeting Hsp90aa (12). Furthermore, miR-195 was reported to increase cardiomyocyte apoptosis mainly by binding the 3' untranslated region (UTR) of Bcl-2 after cardiac ischemia reperfusion (CIR) injury (13). Similarly, miR-106b and miR-15b have been found to regulate apoptosis and angiogenesis in myocardial infarction (14). Hence, miRNAs play a key role in the apoptotic regulatory network. Further elucidating miRNAs and their targets in the cardiomyocyte apoptosis program may shed light on the prevention and treatment of MI in the future.

miRNAs are non-coding RNA molecules involved in the post-transcriptional regulation of gene expression (15,16). They have emerged as regulators of ischemic preconditioning and ischemic postconditioning (16,17). miR-29a-3p has been shown to attenuate hypoxic pulmonary hypertension via suppression of pulmonary adventitial fibroblast activation (18). However, little research has been performed to evaluate the role of miR-29a-3p in the progression of MI. In the current study, the authors mainly explored the expression of miR-29a-3p and the underlying mechanism by which miR-29a-3p is involved in the development of CIR injury.

Correspondence to: Dr Jian Zhang, Heart Center, Beijing Chest Hospital, Capital Medical University, 9 Bei Guan, Beijing 101149, P.R. China
E-mail: jianzhang00001@163.com

Materials and methods

Patients. A total of 100 AMI patients were recruited from the Heart Center, Beijing Chest Hospital (Beijing, China) between January2016 and June 2017. The inclusion criteria were chosen according to the universal definition of MI (19). In brief, AMI patients were clinically diagnosed by the expression levels of biochemical markers [cardiac troponin I (cTnI) >0.1 ng/ml; creatine kinase isoenzyme (CK-MB) ≥15IU/l; lactate dehydrogenase 1 (LDH1)/LDH2 ≥1], acute ischemic-type chest pain, electrocardiography (ECG) changes and coronary angiography. The exclusion criteria were as follows: i) Patients with chest pain was caused by trauma, drugs or medical intervention; ii) patients with terminal kidney failure who required dialysis; or iii) Patients who received intravenous thrombolytic before the initial blood samples. Additionally, 100 adult healthy volunteers with normal ECG findings and no history of cardiovascular disease were enrolled during the same period as normal controls. The basic clinical characteristics are listed in Table I.

Whole blood samples were prospectively collected from AMI patients after they were enrolled in the hospital and from healthy controls. Whole blood (5-8 ml) was collected in an ethylenediaminetetraacetic acid (EDTA) tube. The sample was centrifuged twice at 1,500 x g for 15 min at 4°C. The plasma (supernatant after second centrifugation) was then stored at -80°C. The research protocols were approved by the Beijing Chest Hospital and written informed consent was obtained from the participants.

Adenovirus vectors. Adenovirus vectors that overexpressed miR-29a-3p (Ad-miR-29a-3p), inhibited miR-29a-3p (Ad-miR-29a-3pi) or contained a negative control (Ad-NC) were constructed by Shanghai GeneChem Co., Ltd.

Animal treatment. Adult male wild-type C57BL/6 mice (n=12) weighing approximately 18-22 g were purchased from the Animal Center, Central South University (Changsha, China). The mice were housed in a temperature- and humidity-controlled (40%) animal room at 25°C with a 12 h day/dark cycle with free access to food and water. The thoracic cavity of each mouse was opened by a left thoracotomy, and 8-0 prolene sutures were passed under the left anterior descending (LAD) coronary artery located at the inferior edge of the left atrium and tied to produce an occlusion. After LAD coronary artery ligation, the persistent elevation of the ST segment was located. This led to the successful confirmation of the ischemia model. After 30 min of ischemia induction, the ligature was released and the mice were reperfused. Finally, the chest of each mouse was closed with 6-0 prolene sutures and the endotracheal tube was removed to resume spontaneous respiration. In addition, mice in the sham group (n=4) underwent a similar operation, except the ligation of the LAD coronary artery was not performed. Mice were then split into two groups: i) The CIR+Ad-NC group (n=4), who underwent ischemia induction for 30 min followed by 12 h reperfusion and were injected once with Ad-NC ($2x10^{11}$ viral genome particle per mouse heart) into the left ventricular cavity of mice through the heart apex for 48 h; ii) the CIR+Ad-miR-29a-3pi group (n=4), who underwent ischemia induction for 30 min followed by 12 h reperfusion

and were then injected once with Ad-miR-29a-3pi ($2x10^{11}$ viral genome particle per mouse heart) into the left ventricular cavity of mice through the heart apex for 48 h. A total of 5, 7 and 10 days after the injections, mice were assessed using an echocardiography. At the time of sacrifice, anesthesia was induced by isoflurane (Beijing Solarbio Science and Technology Co., Ltd.; 3% induction, 1.5% maintenance). Animal protocols were approved by Beijing Chest Hospital, Capital Medical University and all animal studies were conducted in accordance with the principles and procedures outlined for the Care and Use of Laboratory Animals (20).

Primary cardiomyocyte culture. A total of 3 parental female 8-week-old C57BL/6 mice (weight, ~18-22 g; Animal Center of Central South University, Changsha, China) were used to produce neonates, from which neonatal hearts at 1-3 days of age were isolated and cultured as previously described (21). Parental and neonatal mice were housed in a temperature- and humidity-controlled (40%) room at 25°C with a 12 h light/dark cycle and free access to food and water. In brief, 1-3-day-old neonatal hearts from 10 male neonates weighing ~1.5-3 g were minced and digested with collagenase type II (Worthington) solution (Sigma-Aldrich; Merck KGaA). Then, the digested cells were plated for 2 h to enrich for cardiomyocytes in Dulbecco's modified Eagle's medium supplemented with 10% fetal bovine serum, 100 U/ml penicillin and 100 µg/ml streptomycin (all GE Healthcare Life Sciences) at 37°C in a humidified atmosphere containing 5% CO_2. After the incubation, the attached cells were considered as non-myocytes and discarded, while the unattached cells were considered to be primarily cardiomyocytes.

Plasma RNA isolation. Total RNA from whole blood samples or heart tissue samples was isolated using RNAVzol LS or RNAVzol (both Vigorous Biotechnology Beijing Co., Ltd.), respectively, according to the manufacturer's protocol to isolate small RNAs. Briefly, 500 µl whole blood samples or 10 mg heart tissue samples were mixed with 500 µl RNAVzol LS or RNAVzol, respectively. The mixture was incubated at room temperature for 15 min. Then, 200 µl chloroform was added and incubated with the above mixture for 5 min. After that, the mixture was centrifuged at 11,000 x g for 10 min at 4°C. The supernatant was collected and 500 µl dimethyl carbinol was added. The supernatant mixture was then incubated at 4°C overnight. After that, the mixture was centrifuged at 11,000 x g for 10 min at 4°C and the precipitate was retained. Finally, 10 µl diethyl pyrocarbonate-treated water (Beijing Solarbio Science and Technology Co., Ltd.) was added to dissolve the precipitate. The quality, quantity and integrity of RNA were monitored using a NanoDrop spectrophotometer (ND-1000; Thermo Fisher Scientific, Inc.).

Reverse transcription-quantitative (RT-q)PCR validation. A total of 1 µg RNA was reverse transcribed using 1 µl Moloney Murine Leukemia Virus reverse transcription enzyme (Applied Biosystems; Thermo Fisher Scientific, Inc.) with specific primers. The detailed RT-qPCR procedure was as follows: 95°C for 10 min followed by 50 cycles of 95°C for 10 sec, 55°C for 10 sec, 72°C for 5 sec, 99°C for 1 sec, and then cooling to 4°C. To quantify the relative mRNA levels, qPCR was performed

Table I. Clinical characteristics of all the patients.

Characteristic	Healthy control (n=100)	AMI (n=100)	P-value
Age (years)	63.57±12.57	64.78±11.68	0.346
Sex (male/female)	56/44	48/52	0.532
Hypertension (%)	54	55	0.432
Hyperlipidemia (n)	57	38	0.547
TC (mg/dl)	3.68±0.12	4.12±0.09	0.047
TG (mg/dl)	1.58±0.10	1.69±0.14	0.132
HDL (mg/dl)	1.22±0.06	1.07±0.04	0.032
LDL (mg/dl)	2.46±0.08	2.66±0.11	0.324
Body mass index (kg/m^2)	23.01±2.68	23.87±2.89	0.165
CK-MB (IU/l)	18.65±4.56	82.34±111.25	0.0001
cTnI (μg/l)	0.23±0.25	17.45±32.56	0.0001

AMI, acute myocardial infarction; TC, total cholesterol; TG, total triglyceride; HDL, high density lipoprotein; LDL, low density lipoprotein; cTnI, cardiac troponin I; CK-MB, creatine kinase-muscle/brain.

using SYBR Green Supermix in an iCycler iQ™ Real-Time PCR Detection system (both Bio-Rad Laboratories, Inc.). The PCR amplifications were performed in a 10-μl reaction system containing 5 μl SYBR Green Supermix, 0.4 μl forward primer, 0.4 μl reverse primer, 2.2 μl double distilled H$_2$O and 2 μl template cDNA. Thermocycling conditions were as follows: 95˚C for 10 min followed by 40 cycles of 95˚C for 15 sec and 60˚C for 1 min. Relative mRNA expression was normalized to U6 using the 2$^{-\Delta\Delta Cq}$ method (22). Primer sequences are as follows: miR-29a-3p-RT, 5-GTCGTATCCAGTGCAGGGTCC GAGGTATTCGCACTGGATACGATAACCG-3'; U6-RT, 5'-GTCGTATCCAGTGCAGGGTCCGAGGTATTCGCACTG GATACGACAAAATG-3'; miR-29a-3p, forward 5'-CGTAGC ACCATCTGAAATCG-3'; U6, forward 5'-GCGCGTCGTGAA GCGTTC-3'; universal reverse primer, 5'-GTGCAGGGTCCG AGGT-3'.

Protein extraction and western blot analysis. Protein samples were extracted from primary cardiomyocytes in radioimmuno-precipitation assay buffer (1% Triton X-100, 15 mmol/l NaCl, 5 mmol/l EDTA and 10 mmol/l Tris-HCl, pH 7.0; Beijing Solarbio Science and Technology Co., Ltd.) supplemented with a protease and phosphatase inhibitor cocktail (Sigma-Aldrich; Merck KGaA). A bicinchoninic protein assay kit (Pierce; Thermo Fisher Scientific, Inc.) was used to determine the protein concentration. Equal quantities of protein (15 μg/lane) were separated by SDS-PAGE on a 10% gel and electrophoretically transferred to a PVDF membrane. Following blocking with 8% milk in PBS with 1% Tween-20 (PBST, pH 7.5) for 2 h at room temperature, membranes were incubated with the following primary antibodies at 4˚C overnight: Anti-Akt (cat. no. 4691), anti-phosphorylated (p-)Akt (Thr308; cat. no. 13038), anti-p38 mitogen-activated protein kinase (p38; cat. no. 8690), anti-p-p38 (cat. no. 4511), anti-cleaved-caspase-3 (cat. no. 9664), and anti-GAPDH (cat. no. 5174) (all Cell Signaling Technology, Inc.; 1:5,000). Following several washes with TBST, the membranes were incubated with horseradish peroxidase (HRP)-conjugated goat anti-rabbit IgG (1:5,000; cat. no. ZB-2301; OriGene Technologies,

Inc.) for 2 h at room temperature and then washed in 1% PBST. Immunodetection was performed using the Pierce™ ECL Plus Western Blotting Substrate (cat. no. WBKLS0050; Thermo Fisher Scientific, Inc.) according to the manufacturer's protocol. The housekeeping gene GAPDH was used as the internal control. ImageJ 1.43b software (National Institutes of Health) was used for density analysis.

Luciferase target assay. According to TargetScan 7.2 (http://www.targetscan.org/vert_72/), a conserved binding site of miR-29a-3p was found in the 3'UTR of Bax. The 3'UTR of Bax containing the predicted binding site of miR-29a-3p was cloned into the pmirGLO firefly luciferase reporter vector (Promega Corporation). The PCR procedures were as follows: A hot start step at 95˚C for 10 min, 40 cycles at 95˚C for 15 sec and 55˚C for 45 sec, then a final step of 72˚C for 30 sec.

For the luciferase reporter assay, cells were seeded at 5x10^4 cells/well in 24-well plates in 500 μl DMEM (HyClone; GE Healthcare Life Sciences) supplemented with 10% FBS (HyClone; GE Healthcare Life Sciences), 100 U/ml penicillin (HyClone; GE Healthcare Life Sciences) and 100 μg/ml streptomycin (HyClone; GE Healthcare Life Sciences) for 18 h at 37˚C. Then, the modified firefly luciferase vector (500 ng/μl) was mixed with Vigofect transfection reagent (Vigorous Biotechnology Beijing Co., Ltd.) according to the manufacturer's protocol. After transfection for 48 h, the Dual-luciferase Reporter Assay system (Promega Corporation) was applied to determine the changes in relative light units caused by the luciferase activity. *Renilla* luciferase activity was used to normalize the firefly luciferase activity.

Two-dimensional echocardiography. Two-dimensional echocardiography of the mice was performed as previously reported (23). For the evaluation, the mice were anesthetized and the chest was shaved. Next, an ultrasound system (model no. SSD-900; Hitachi Aloka Medical, Ltd.) was used to perform two-dimensional echocardiography. To determine the papillary muscle level of the left ventricle (LV), two-dimensional

short-axis images were taken. A single observer was responsible for the examination of end-diastolic posterior wall thickness, and end-diastolic and end-systolic internal diameters of the LV.

The calculation of relative wall thickness (RWT) was calculated as follows:

$$RWT = 2 \times LVPWTd/LVDd,$$

Here, LVPWTd is the end-diastolic posterior wall thickness of the LV, while LVDd refers to an end-diastolic internal diameter of the LV.

The calculation of fractional shortening (FS) was as follows:

$$FS = 100 \times (LVDd - LVDs)/LVDd$$

LVDs refers to the end-systolic internal diameter of the LV.

Hoechst 33258 staining. To determine the effects of the Ad-miR-29a-3p inhibitor on cell apoptosis, primary cardiomyocytes were cultured in six-well plates at a density of 10^6 cells/well for 24 h. Samples were subsequently infected with Ad-miR-29a-3pi or Ad-NC (density, 10^7 viral genome particles) for 48 h at 37°C. The cells were washed with PBS three times (5 min/time) and stained with Hoechst 33258 (Beijing Solarbio Science and Technology Co., Ltd.) for 5 min. Next, the cells were washed with PBS three times (5 min/time) and observed under a fluorescence microscope (magnification, x40; Olympus Corporation).

Apoptosis assay. Primary cardiomyocytes were cultured in six-well plates at a density of 10^6 cells/well for 24 h and infected with Ad-miR-29a-3pi or Ad-NC (density, 10^7 viral genome particles) for 48 h at 37°C. Then, the cells were collected and washed with PBS three times (5 min/time). To determine cell apoptosis, an Annexin V-FITC-propidium iodide (PI) Apoptosis kit (Invitrogen; Thermo Fisher Scientific, Inc.) was used. In brief, the cells were washed with 1X Annexin V Binding Buffer (140 mM NaCl, 2.5 mM $CaCl_2$ and 10 mM HEPES/NaOH, pH 7.4) at a concentration of $2\text{-}3\times10^6$ cells/ml. Then, the Annexin V-FITC and PI buffer was added and incubated with the cells at room temperature for 15 min. After treatment, the cells were filtered using a 300-mesh filter and analyzed by a BD FACSCalibur system (BD Biosciences) within 1 h of staining. Data were analyzed using ModFit software version 4.1 (Verity Software House, Inc.).

Determination of reactive oxygen species (ROS). Primary cardiomyocytes were cultured in six-well plates at a density of 10^6 cells/well for 24 h and were infected with Ad-miR-29a-3pi or Ad-NC (density, 10^7 viral genome particles) for 48 h at 37°C. The cells were collected and washed with PBS three times (5 min/time). Afterwards, the cells were incubated with ROS Fluorescent Probe-dihydroethidium (DHE; Vigorous Biotechnology Beijing Co., Ltd.) in serum-free DMEM:Ham's F12 Nutrient Mixture medium for 30 min at 37°C in darkness. Then, the cells were fixed in 4% paraformaldehyde for 30 min at room temperature and the slides were mounted. The fluorescence was examined by fluorescent microscopy (magnification, x40; Olympus Corporation). To quantify the relative fluorescence, the cells stained with Probe-DHE were collected at a concentration of 2.5×10^6 cells/ml and analyzed using a BD FACSCalibur system (BD Biosciences) within 1 h of staining. Data were analyzed using ModFit software version 4.1 (Verity Software House, Inc.).

Determination of caspase-3 activity. A Caspase 3 Activity Assay kit (Beyotime Institute of Biotechnology) was applied to determine the activity of caspase-3 in accordance with the manufacturer's protocol. In brief, Primary cardiomyocytes were cultured in six-well plates at a density of 10^6 cells/well for 24 h and infected with Ad-miR-29a-3pi or Ad-NC (density, 10^7 viral genome particles) for 48 h at 37°C. Cells were treated with the lysates included in the Caspase 3 Activity Assay kit. Subsequently, the lysates from primary cardiomyocytes were collected and incubated with the substrates from the kit for 1 h at 37°C. To determine the enzyme activity, the intensity of fluorescence was measured by a spectrophotometer. The activity was calculated by comparing with the level of fluorescence in the treated groups with the untreated control.

Statistical analysis. The data are presented as mean ± standard error of the mean. Two-tailed unpaired Student's t-tests were used for comparisons of two groups. The one-way analysis of variance multiple comparison test followed by a Turkey post hoc test were used for comparisons of more than two groups. The receiver operating characteristic (ROC) curve analysis was used to assess miR-29a-3p as a biomarker and the area under the curve (AUC) was found using SPSS software (version 20.0; IBM Corp.). $P<0.05$ was considered a statistically significant difference.

Results

miR-29a-3p levels are higher in mice with CIR injury and reduction of miR-29a-3p enhances ROS production in primary cardiomyocytes. First, the level of miR-29a-3p in the hearts of CIR mice were evaluated. Compared with the sham group, the level of miR-29a-3p was significantly decreased in the hearts of CIR mice (Fig. 1A). DHE staining showed that intracellular ROS content was significantly increased in primary cardiomyocytes transfected with Ad-miR-29a-3pi compared with those transfected with Ad-NC (Fig. 1B).

Inhibition of miR-29a-3p induces primary cardiomyocyte apoptosis. Then, the effect of miR-29a-3p on cardiomyocyte apoptosis was evaluated. Hoechst staining demonstrated that the number apoptotic cells were increased after infection with Ad-miR-29a-3pi in primary cardiomyocytes compared with those infected with Ad-NC (Fig. 2A). Meanwhile, flow cytometry analysis showed that the inhibition of miR-29a-3psignificantly increased cardiomyocyte apoptosis ~3-fold compared with the control (Fig. 2B). The authors of the current study also determined the activity of caspase-3. Compared with Ad-NC, infection with Ad-miR-29a-3pi significantly increased caspase-3 activity at 16 and 24 h in what appears to be a time-dependent manner (Fig. 2C). These data indicated that inhibition of miR-29a-3p increased cardiomyocyte apoptosis.
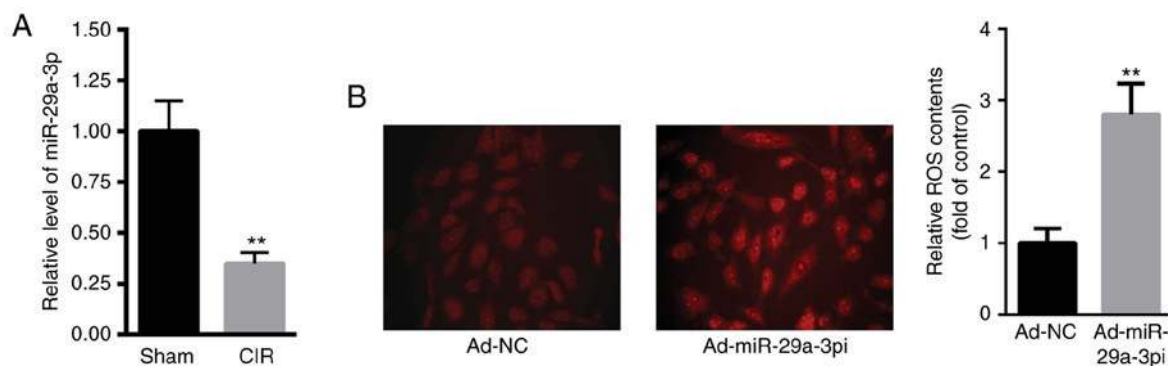
Figure 1. miR-29a-3p levels are higher in mice with CIR injury and reduction of miR-29a-3p enhances ROS production in primary cardiomyocytes. (A) miR-29a-3p levels of in the hearts of CIR injury mice. (B) ROS content in primary cardiomyocytes (magnification, x40). Data were presented as mean ± standard error of the mean. n=5. **P<0.01 vs. respective controls. miR, microRNA; ROS, reactive oxygen species; CIR, cardiac ischemia reperfusion; NC, negative control.
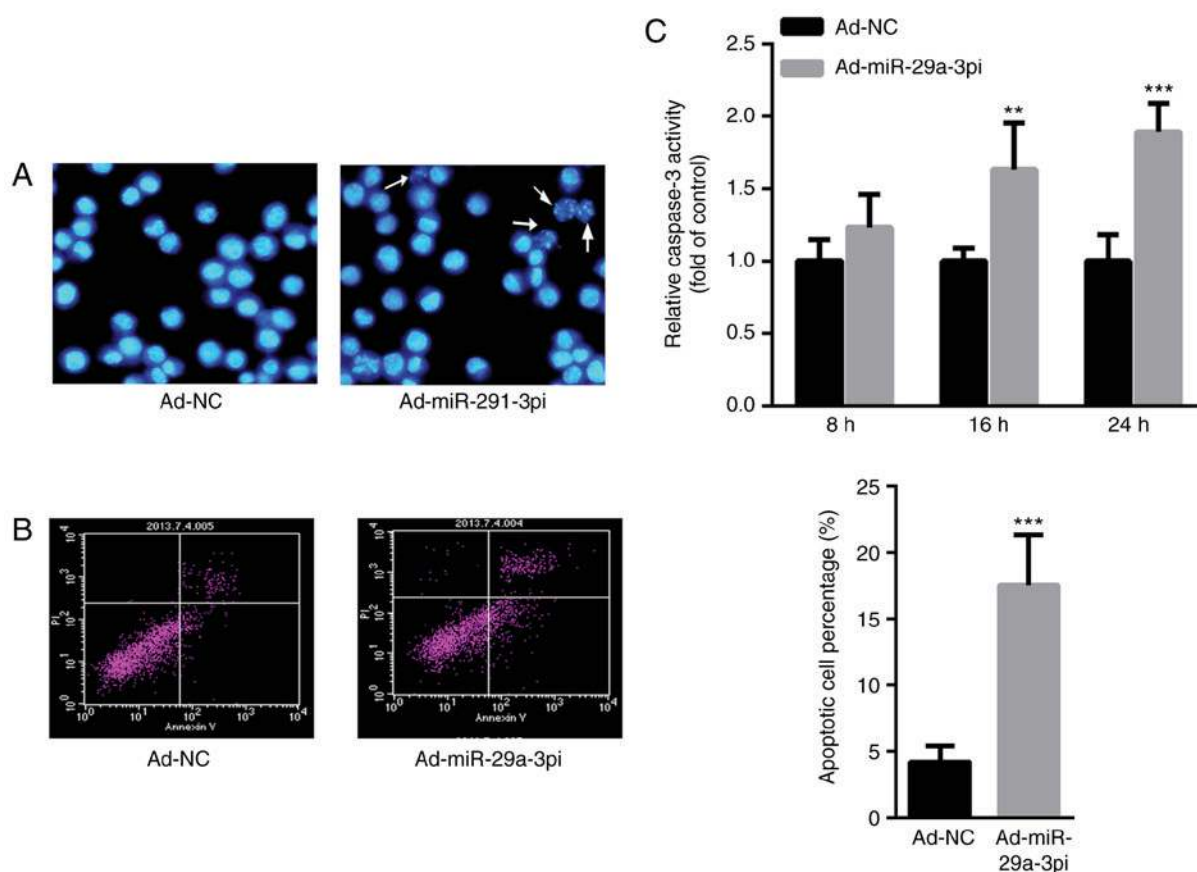

Figure 2. Inhibition of miR-29a-3p increases capcase-3 activity and induces primary cardiomyocyte apoptosis. (A) Hoechst staining (magnification, x40) and (B) flow cytometry analysis of primary cardiomyocytes. White arrows indicate apoptotic cells. (C) Capcase-3 activity in primary cardiomyocytes. Data were presented as mean ± standard error of the mean. n=3. **P<0.01 and ***P<0.001 vs. Ad-NC. miR, microRNA; NC, negative control.

Cardiac function is impaired in ischemic hearts, and Akt and p38 phosphorylation is decreased in primary cardio-myocytes after inhibition of miR-29a-3p. Moreover, cardiac function after mice with CIR injury were injected with Ad-miR-29a-3pi or Ad-NC was also evaluated. As shown in Fig. 3A, left ventricular FS was significantly decreased in mice after 7 and 10 days post-injection with Ad-miR-29a-3pi compared with mice that received Ad-NC. Similarly, RWT was significantly decreased in the hearts of mice infected with Ad-miR-29a-3pi compared with mice that received

Ad-NC after 7 and 10 days (Fig. 3B). Inactivation of p38 and the Akt signaling pathway is suggested to be pro-apoptotic in the process of MI (24). Hence, the phosphorylation levels of p38 and Akt were evaluated in ischemic hearts after infection with Ad-miR-29a-3pi. The data showed that the activation of Akt and p38 was significantly decreased when miR-29a-3p was inhibited (Fig. 3C).

Bax is the target gene of miR-29a-3p. Based on the above findings, the possible target genes of miR-29a-3p
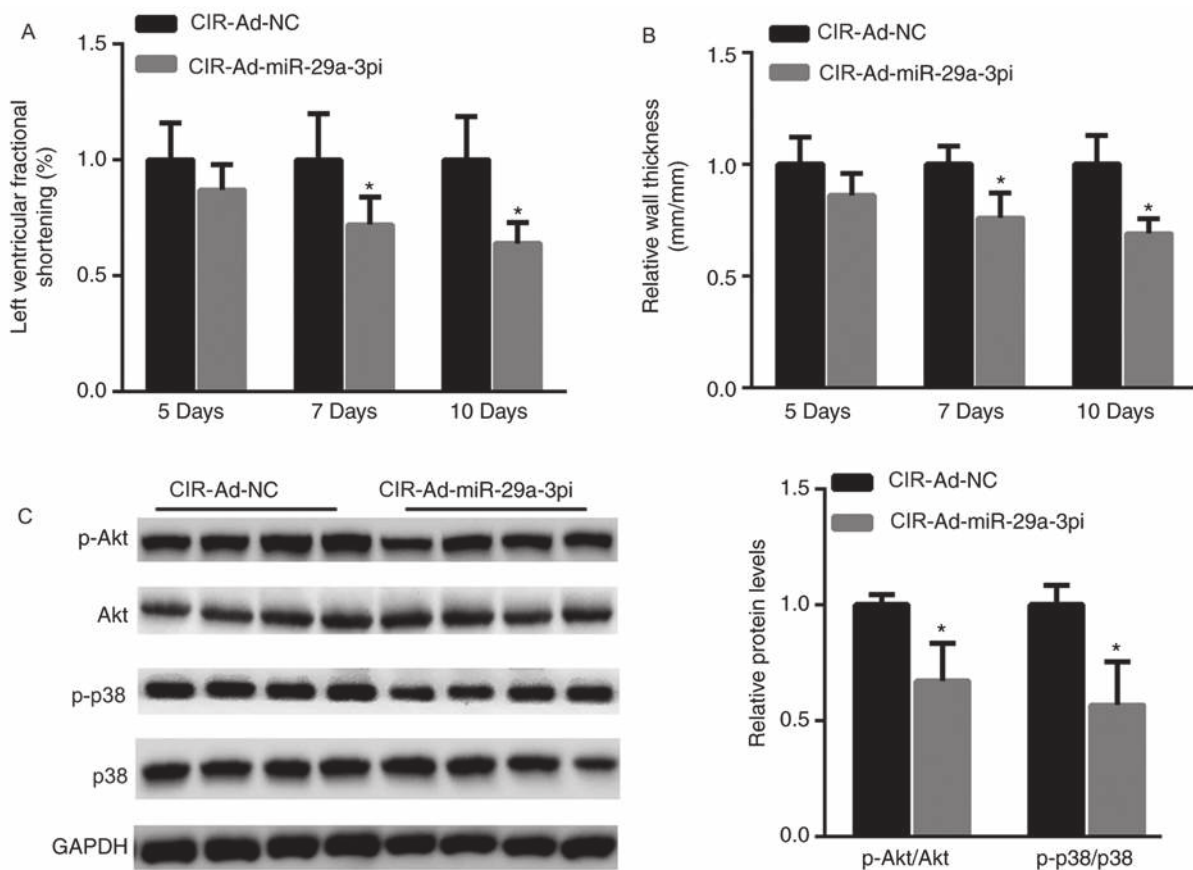
Figure 3. Cardiac function is impaired in ischemic hearts, and Akt and p38 phosphorylation is decreased in primary cardiomyocytes after inhibition of miR-29a-3p. (A) Left ventricular fractional shortening and (B) relative wall thickness in CIR injury mice 5, 7 and 10 days after injections. (C) Western blotting and quantification of proteins in primary cardiomyocytes. Data were presented as mean ± standard error of the mean. n=5. *P<0.05 vs. respective controls. miR, microRNA; NC, negative control; Ad, adenovirus vector; Ad-miR-29a-3pi, adenovirus inhibiting miR-29a-3p; CIR, cardiac ischemia reperfusion.

in cardiomyocyte apoptosis were explored. According to TargetScan 7.2 (http://www.targetscan.org/vert_72/), a conserved binding site of miR-29a-3p was found in the 3'UTR of Bax, an important pro-apoptosis member of Bcl2 family (25) (Fig. 4A). Dual luciferase reporter assay showed that Ad-miR-29a-3pi significantly suppressed the relative luciferase activity of pmirGLO-Bax-3'UTR compared with the blank pmirGLO plasmid (Fig. 4B). Meanwhile, overexpression of miR-29a-3p significantly suppressed the protein level of Bax in primary cardiomyocytes compared with the control (Fig. 4C). In contrast, inhibition of miR-29a-3p increased the expression of Bax in primary cardiomyocytes with the control (Fig. 4D). These data indicated that lower miR-29a-3p levels increased primary cardiomyocyte apoptosis by targeting Bax.

miR-29a-3p expression increases in AMI patients. The level of miR-29a-3p in the plasma of 100 AMI patients and 100 healthy controls was measured. Compared with healthy controls (36.74±13.78), circulating miR-29a-3p was significantly decreased in AMI patients (1.00±0.21; Fig. 5A). To investigate whether miR-29a-3p could be used as a potential biomarker for AMI patients, ROC curve analysis was carried out. The data showed that miR-29a-3p may be able to screen AMI patients from healthy controls, with an AUC of 0.87 [95% confidence interval (CI), 0.81-0.93; data not shown], which was comparable

to cTnI, which has an AUC of 0.92 (95% CI, 0.78-0.89; data not shown), and CK-MB, which has an AUC of 0.84 (95% CI, 0.78-0.83; data not shown). These observations indicate that miR-29a-3p could be a good biomarker that can be measured in the plasma of AMI patients.

Discussion

MicroRNAs play an important role in myocardial infarction by regulating apoptotic, necrotic and autophagic cell death. Multiple aberrantly expressed miRNAs have been implicated in the progression of myocardial infarction, including miR-29a, let-7, miR-34 and miR-130a (26-28). To the best of our knowledge, the current study is the first to show that the level of miR-29a-3p was reduced in the hearts of CIR injury mice compared with those of control mice. Further study showed that the inhibition of miR-29a-3p could increase the production of ROS. Oxidative stress is detrimental, and has been widely accepted to cause CIR injury and enhance ROS production, thereby triggering cell apoptosis (29,30).

Hence, the author evaluated the role of miR-29a-3p on primary cardiomyocyte apoptosis. The data showed that inhibition of miR-29a-3p significantly increased primary cardiomyocyte apoptosis, suggesting a detrimental effect of miR-29a-3p after CIR injury in mice. Previous studies have indicated that the activation of p38 and Akt is associated with
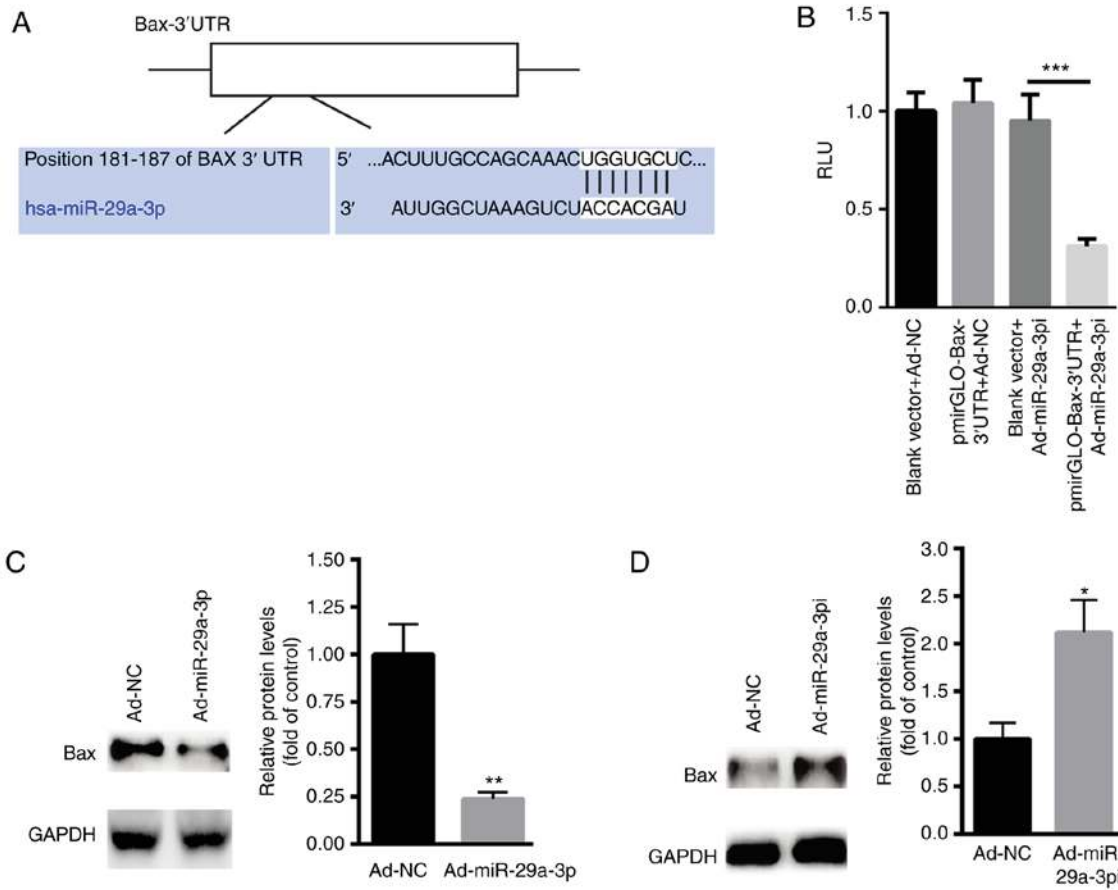
Figure 4. Bax is the target gene of miR-29a-3p. (A) Schematic analysis of the binding site of miR-29a-3p on the 3'UTR of Bax. (B) Dual luciferase reporter assay following the co-transfections of pmirGLO-Bax or pmirGLO with Ad-miR-29a-3pi or Ad-NC. Western blotting and quantification of Bax protein expression after transfecting cells with Ad-NC and (C) Ad-miR-29a-3pi or (D) Ad-miR-29a-3p in primary cardiomyocytes. Data were presented as mean ± standard error of the mean. n=5. *P<0.05, **P<0.01 and ***P<0.001 vs. respective Ad-NCs. UTR, untranslated region; miR, microRNA; NC, negative control; Ad, adenovirus vector; Ad-miR-29a-3pi, adenovirus inhibiting miR-29a-3p; Ad-miR-29a-3p, adenovirus overexpression miR-29a-3p; RLU, relative light units.
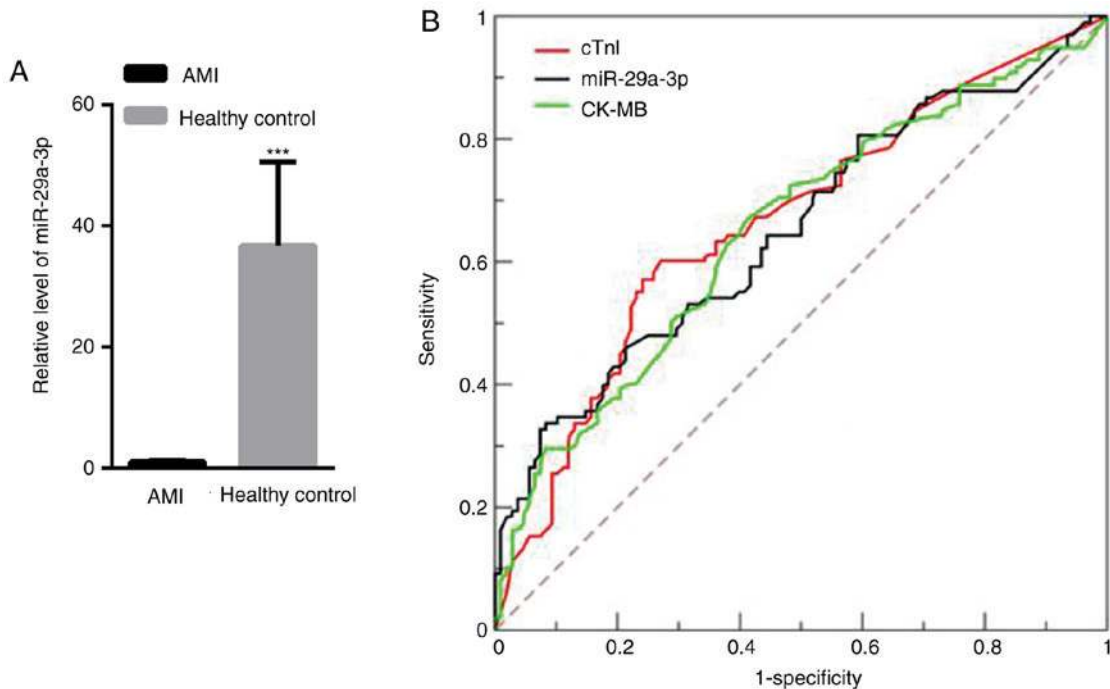

Figure 5. Plasma miR-29a-3p expression increases in AMI patients. (A) miR-29a-3p levels of in healthy controls and AMI patients. (B) Receiver operating characteristic curve analysis of miR-29a-3p, cTnI and CK-MB. ***P<0.001 vs. healthy control. AMI, acute myocardial infarction; miR, microRNA; cTnI, cardiac troponin I; CK-MB, creatine kinase-muscle/brain.

protection induced by ischemia and reperfusion injury (7,19). Therefore, the authors of the current study explored whether inhibition of miR-29a-3p could lead to the inactivation of the p38/Akt signaling pathway. Western blot analysis showed that the inhibition of miR-29a-3p resulted in decreased phosphorylation levels of p38/Akt signaling. These data indicated a cardioprotective role for miR-29a-3p via the activation of p38 and Akt signaling.

The authors further explored the possible target genes of miR-29a-3p. A conserved binding site of miR-29a-3p was found in the 3'UTR of Bax. Bax plays an important role in the Bcl-2 multi-gene family (31), which exerts a pro-apoptotic effect (25). In mice with CIR injury, reduction of Bax may improve CIR injury (32). In the current study, the data showed that overexpression of miR-29a-3p suppressed the expression of Bax, thereby inducing myocardial dysfunction and injury (33). More importantly, the level of plasma miR-29a-3p in AMI patients was also evaluated. The data showed that circulating miR-29a-3p was significantly decreased in the plasma of AMI patients than in that of healthy controls. ROC curve analysis further demonstrated that plasma miR-29a-3p has a considerable diagnostic efficiency, which is comparable to cTnI and CK-MB.

Increasing evidence reveals that miRNAs function as pro- or anti-MI factors via interactions with myocardial cell death and cardiomyocyte regeneration pathways (34,35). At present, significant progress has been made to elucidate the miRNAs-regulated signaling pathways of MI, which has greatly enhanced understanding of CIR injury (36). The most important challenges for miRNA-based therapy are off-target effects in different organs or cell types.

The limitation of the current study is that the small sample size may limit the statistical significance of the study. Therefore, the potential of plasma miR-29a-3p expression as a biomarker of AMI must be confirmed and validated in large populations. Future work will increase the sample size. In addition, regular follow-ups of AMI patients will help to analyze the prognostic value of miR-29a-3p in AMI.

In summary, the authors of the current study presented novel data showing that the level of miR-29a-3p was significantly reduced in the hearts of CIR mice and the plasma of patients with AMI. Further study indicated that the inhibition of miR-29a-3p induced ROS production and apoptosis in primary cardiomyocytes via targeting Bax. The results of the current study may therefore improve the early diagnosis and treatment of patients with AMI in the future.

Acknowledgements

Not applicable.

Funding

The present study was supported by a grant from the Beijing Chest Hospital (BCH-20170512).

Availability of data and materials

The datasets used and/or analyzed during the current study are available from the corresponding author on reasonable request.

Authors' contributions

LZ performed the experiments and analyzed the data. QT, GW, HD, ZW, QS and HW each performed part of the reverse transcription-quantitative PCR experiments. JZ designed the experiments, analyzed the data and gave final approval of the version to be published. All authors read and approved the final manuscript.

Ethics approval and consent to participate

The present study was approved by the Research Ethics Committee of Beijing Chest Hospital (Beijing, China) and all the patients have provided written informed consent for this study.

Patient consent for publication

Informed consent for participation in the study or use of their tissue was obtained from all participants.

Competing interests

The authors declare that they have no competing interests.

References

1. Wu A, Zhao M, Lou L, Zhai J, Zhang D, Zhu H, Gao Y, Shang H and Chai L: Effect of Wenxin granules on gap junction and miR-1 in rats with myocardial infarction. Biomed Res Int 2017: 3495021, 2017.
2. Lin J and Zheng X: Salvianolate blocks apoptosis during myocardial infarction by down regulating miR-122-5p. Curr Neurovasc Res 14: 323-329, 2017.
3. Yan Y, Song X, Li Z, Zhang J, Ren J, Wu J, Li Y, Guan Y and Wang J: Elevated levels of granzyme B correlated with miR-874-3p downregulation in patients with acute myocardial infarction. Biomark Med 11: 761-767, 2017.
4. Yang F, Liu W, Yan X, Zhou H, Zhang H, Liu J, Yu M, Zhu X and Ma K: Effects of mir-21 on cardiac microvascular endothelial cells after acute myocardial infarction in rats: Role of phosphatase and tensin homolog (PTEN)/vascular endothelial growth factor (VEGF) signal pathway. Med Sci Monit 22: 3562-3575, 2016.
5. Yang SY, Wang YQ, Gao HM, Wang B and He Q: The clinical value of circulating miR-99a in plasma of patients with acute myocardial infarction. Eur Rev Med Pharmacol Sci 20: 5193-5197, 2016.
6. Yuan J, Chen H, Ge D, Xu Y, Xu H, Yang Y, Gu M, Zhou Y, Zhu J, Ge T, *et al*: Mir-21 promotes cardiac fibrosis after myocardial infarction via targeting Smad7. Cell Physiol Biochem 42: 2207-2219, 2017.
7. Pan LJ, Wang X, Ling Y and Gong H: miR-24 alleviates cardiomyocyte apoptosis after myocardial infarction via targeting BIM. Eur Rev Med Pharmacol Sci 21: 3088-3097, 2017.
8. Maciejak A, Kiliszek M, Opolski G, Segiet A, Matlak K, Dobrzycki S, Tulacz D, Sygitowicz G, Burzynska B and Gora M: miR-22-5p revealed as a potential biomarker involved in the acute phase of myocardial infarction via profiling of circulating microRNAs. Mol Med Rep 14: 2867-2875, 2016.
9. Roy S, Khanna S, Hussain SR, Biswas S, Azad A, Rink C, Gnyawali S, Shilo S, Nuovo GJ and Sen CK: MicroRNA expression in response to murine myocardial infarction: miR-21 regulates fibroblast metalloprotease-2 via phosphatase and tensin homologue. Cardiovasc Res 82: 21-29, 2009.
10. Li X, Hu H, Wang Y, Xue M, Li X, Cheng W, Xuan Y, Yin J, Yang N and Yan S: Valsartan ameliorates KIR2.1 in rats with myocardial infarction via the NF-κB-miR-16 pathway. Gene 590: 201-209, 2016.
11. Li Y and Maegdefessel L: My heart will go on-beneficial effects of anti-miR-30 after myocardial infarction. Ann Transl Med 4: 144, 2016.

12. Zhu WS, Guo W, Zhu JN, Tang CM, Fu YH, Lin QX, Tan N and Shan ZX: Hsp90aa1: A novel target gene of miR-1 in cardiac ischemia/reperfusion injury. Sci Rep 6: 24498, 2016.

13. Gao CK, Liu H, Cui CJ, Liang ZG, Yao H and Tian Y: Roles of MicroRNA-195 in cardiomyocyte apoptosis induced by myocardial ischemia-reperfusion injury. J Genet 95: 99-108, 2016.

14. Liu Z, Yang D, Xie P, Ren G, Sun G, Zeng X and Sun X: miR-106b and miR-15b modulate apoptosis and angiogenesis in myocardial infarction. Cell Physiol Biochem 29: 851-862, 2012.

15. Kaija H, Pakanen L and Porvari K: RNU6B, a frequent reference in miRNA expression studies, differentiates between deaths caused by hypothermia and chronic cardiac ischemia. Int J Legal Med, 2019.

16. Zhou Y, Chen Q, Lew KS, Richards AM and Wang P: Discovery of potential therapeutic miRNA targets in cardiac ischemia-reperfusion injury. J Cardiovasc Pharmacol Ther 21: 296-309, 2016.

17. Tu Y, Wan L, Fan Y, Wang K, Bu L, Huang T, Cheng Z and Shen B: Ischemic postconditioning-mediated miRNA-21 protects against cardiac ischemia/reperfusion injury via PTEN/Akt pathway. PLoS One 8: e75872, 2013.

18. Luo Y, Dong HY, Zhang B, Feng Z, Liu Y, Gao YQ, Dong MQ and Li ZC: miR-29a-3p attenuates hypoxic pulmonary hypertension by inhibiting pulmonary adventitial fibroblast activation. Hypertension 65: 414-420, 2015.

19. Thygesen K, Alpert JS and White HD; Joint ESC/ACCF/AHA/WHF Task Force for the Redefinition of Myocardial Infarction: Universal definition of myocardial infarction. Eur Heart J 28: 2525-2538, 2007.

20. Chen L, Ji Q, Zhu H, Ren Y, Fan Z and Tian N: miR-30a attenuates cardiac fibrosis in rats with myocardial infarction by inhibiting CTGF. Exp Ther Med 15: 4318-4324, 2018.

21. Parameswaran S, Santhakumar R, Vidyasekar P and Verma RS: Enrichment of cardiomyocytes in primary cultures of murine neonatal hearts. Methods Mol Biol 1299: 17-25, 2015.

22. Livak KJ and Schmittgen TD: Analysis of relative gene expression data using real-time quantitative PCR and the 2(-Delta Delta C(T)) Method. Methods 25: 402-408, 2001.

23. Cittadini A, Strömer H, Katz SE, Clark R, Moses AC, Morgan JP and Douglas PS: Differential cardiac effects of growth hormone and insulin-like growth factor-1 in the rat. A combined in vivo and in vitro evaluation. Circulation 93: 800-809, 1996.

24. Xie Q, Sun Z, Chen M, Zhong Q, Yang T and Yi J: IL-8 up-regulates proliferative angiogenesis in ischemic myocardium in rabbits through phosphorylation of Akt/GSK-3β(ser9) dependent pathways. Int J Clin Exp Med 8: 12498-12508, 2015.

25. Li T, Chen L, Yu Y, Yang B, Li P and Tan XQ: Resveratrol alleviates hypoxia/reoxygenation injury-induced mitochondrial oxidative stress in cardiomyocytes. Mol Med Rep 19: 2774-2780, 2019.

26. Wang L, Niu X, Hu J, Xing H, Sun M, Wang J, Jian Q and Yang H: After myocardial ischemia-reperfusion, miR-29a, and Let7 could affect apoptosis through regulating IGF-1. Biomed Res Int 2015: 245412, 2015.

27. Joshi S, Wei J and Bishopric NH: A cardiac myocyte-restricted Lin28/let-7 regulatory axis promotes hypoxia-mediated apoptosis by inducing the AKT signaling suppressor PIK3IP1. Biochim Biophys Acta 1862: 240-251, 2016.

28. Lu C, Wang X, Ha T, Hu Y, Liu L, Zhang X, Yu H, Miao J, Kao R, Kalbfleisch J, et al: Attenuation of cardiac dysfunction and remodeling of myocardial infarction by microRNA-130a are mediated by suppression of PTEN and activation of PI3K dependent signaling. J Mol Cell Cardiol 89: 87-97, 2015.

29. Xu J, Qian J, Xie X, Lin L, Zou Y, Fu M, Huang Z, Zhang G, Su Y and Ge J: High density lipoprotein protects mesenchymal stem cells from oxidative stress-induced apoptosis via activation of the PI3K/Akt pathway and suppression of reactive oxygen species. Int J Mol Sci 13: 17104-17120, 2012.

30. Muzi-Filho H, Bezerra CG, Souza AM, Boldrini LC, Takiya CM, Oliveira FL, Nesi RT, Valença SS, Einicker-Lamas M, Vieyra A, et al: Undernutrition affects cell survival, oxidative stress, Ca²⁺ handling and signaling pathways in vas deferens, crippling reproductive capacity. PLoS One 8: e69682, 2013.

31. Liu Z, Li Z and Liu X: Effect of ginsenoside Re on cardiomyocyte apoptosis and expression of Bcl-2/Bax gene after ischemia and reperfusion in rats. J Huazhong Univ Sci Technolog Med Sci 22: 305-309, 2002.

32. Tian Y, Zhang W, Xia D, Modi P, Liang D and Wei M: Postconditioning inhibits myocardial apoptosis during prolonged reperfusion via a JAK2-STAT3-Bcl-2 pathway. J Biomed Sci 18: 53, 2011.

33. Khan M, Meduru S, Mostafa M, Khan S, Hideg K and Kuppusamy P: Trimetazidine, administered at the onset of reperfusion, ameliorates myocardial dysfunction and injury by activation of p38 mitogen-activated protein kinase and Akt signaling. J Pharmacol Exp Ther 333: 421-429, 2010.

34. Wang KJ, Zhao X, Liu YZ, Zeng QT, Mao XB, Li SN, Zhang M, Jiang C, Zhou Y, Qian C, et al: Circulating miR-19b-3p, miR-134-5p and miR-186-5p are promising novel biomarkers for early diagnosis of acute myocardial infarction. Cell Physiol Biochem 38: 1015-1029, 2016.

35. Wienbergen H, Schiele R, Gitt AK, Schneider S, Heer T, Gottwik M, Gieseler U, Weber MA, Müller CH, Neubaur J, et al: Incidence, risk factors, and clinical outcome of stroke after acute myocardial infarction in clinical practice. MIR and MITRA Study Groups. Myocardial Infarction Registry. Maximal Individual Therapy in Acute Myocardial Infarction. Am J Cardiol 87: 782-785, A8, 2001.

36. Xin Y, Yang C and Han Z: Circulating miR-499 as a potential biomarker for acute myocardial infarction. Ann Transl Med 4: 135, 2016.